

# Integer filling metal insulator transitions in the degenerate Hubbard model

Marcelo J. Rozenberg

*Laboratoire de Physique Théorique de l'École Normale Supérieure,  
24, rue Lhomond, 75231 Paris Cedex 05, France.*

*e-mail: marcelo@physique.ens.fr*

(October 6, 2018)

We obtain exact numerical solutions of the degenerate Hubbard model in the limit of large dimensions (or large lattice connectivity). Successive Mott-Hubbard metal insulator transitions at integer fillings occur at intermediate values of the interaction and low enough temperature in the paramagnetic phase. The results are relevant for transition metal oxides with partially filled narrow degenerate bands.

71.27.+a, 71.30.+h, 71.20.Ad

The understanding of strongly correlated electron systems is one of the current challenges in condensed matter physics. In recent years, this problem has received a great deal of attention from theorists and experimentalist alike. Yet, our knowledge of even some of the basic features of the proposed model Hamiltonians remains to a large extent only partial, except, perhaps, in the one-dimensional case. In consequence, the interpretation of the experimental data of strongly correlated electron systems has to remain only speculative in most of the cases. In regard of this situation, exact results on properties of model Hamiltonians in well defined limits is very desirable. The relevant role played by the band degeneracy in models of strongly correlated electrons has been long and largely recognized [1–4]. However, the systematic treatment of such models poses in general even greater technical difficulties than non-degenerate ones. This particularly applies to numerical approaches which have to deal with the exponential grow of the Hilbert space.

The goal of this paper is to demonstrate the existence of successive metal insulator transitions (MIT) at the integer fillings  $n = 1, 2, 3$  in the two band degenerate Hubbard model within the “Local impurity self-consistent approximation” (LISA) [5] which is exact in the limit of large dimensions (or large lattice connectivity) [6]. These MIT occur within the paramagnetic phase for intermediate values of the interaction. We obtain exact numerical solutions of the model using an extension of the Hirsch and Fye quantum Monte Carlo (HFQMC) algorithm [7,8] for the solution of the associated impurity problem within the LISA. This impurity problem is a generalized single impurity Anderson model where the impurity and conduction band operators carry an orbital index.

The two band degenerate Hubbard model reads,

$$H = \sum_{\langle ij \rangle, a, b} t_{ij}^{ab} c_{ia\sigma}^\dagger c_{jb\sigma} + \frac{(U+J)}{2} \sum_{i, a, \sigma} n_{ia\sigma} n_{ia-\sigma} + \frac{U}{2} \sum_{i, a \neq b, \sigma} n_{ia\sigma} n_{ib-\sigma} + \frac{(U-J)}{2} \sum_{i, a \neq b, \sigma} n_{ia\sigma} n_{ib\sigma}$$

$$- \frac{J}{2} \sum_{i, a \neq b, \sigma} c_{ia\sigma}^\dagger c_{ia-\sigma} c_{ib-\sigma}^\dagger c_{ib\sigma} \quad (1)$$

$\langle ij \rangle$  labels nearest neighbor sites and  $a, b = 1, 2$  is the orbital index. This Hamiltonian is rotational invariant in spin and real space and the usual approximation  $U$  and  $J$  independent of band indices is assumed [9]. The parameter  $U$  is due to on-site Coulomb repulsion and the exchange parameter  $J$  originates the Hund’s coupling. For simplicity, we shall further assume  $t_{ij}^{ab} = -t\delta_{ab}$  and neglect the last “spin flip” term in (1). The resulting model Hamiltonian is relevant for electronic systems with partially filled narrow degenerate bands. Examples of such systems are the 3d transition metal oxides  $R_{1-x}A_xMO_3$  with three-dimensional perovskite-type structure, where  $R = La, Y$ ,  $A = Ca, Sr$  and the transition metal  $M = Ti, V, Cr$ . Fujimori has constructed a phase diagram by classifying these compounds as correlated metals or Mott insulators according to their electronic properties [10]. Another and particularly notable example is the extensively investigated  $V_2O_3$  compound which has a MIT as a function of temperature, pressure and chemical substitution [11]. It is important to note that in bipartite lattices such as the hypercubic or the Bethe lattice the groundstate of the model has long range order [3]. In the single band case it is a spin antiferromagnetic (Néel) state, while in the degenerate model (with  $J \approx 0$ ) one can have either a spin ordered and/or an orbital ordered state. Other types of orderings are also a priori possible, as for instance, ferromagnetic (for large  $J$ ). The stability of the different phases will depend on the values of the various interaction parameters appearing in the Hamiltonian (1). Since the parameter space is rather large, we defer the investigation of the full phase diagram for a later publication. Here we choose to concentrate on the interesting question of the destruction of a metallic state by the sole effect of electronic correlations (Mott transition). Therefore, we shall restrict ourselves to the paramagnetic phase (in both spin and orbit indices). It is important to note, however, that the paramagnetic solutions that we obtain are indeed the true groundstate in models that include next nearest neighbor

hopping (that lifts the rather artificial nesting property) and also in models with hopping disorder [12,13].

In this paper we shall consider the model on a Bethe lattice of connectivity  $z \rightarrow \infty$  which renders a semicircular bare density of states  $\rho^o(\epsilon) = (2/\pi D)\sqrt{1 - (\epsilon/D)^2}$ , with  $D = 2t$ . Our choice is motivated from the fact that  $\rho^o(\epsilon)$  shares common features with a realistic three dimensional cubic tight binding model, namely, it is bounded and has the same square root behavior at the edges. We shall set the half-bandwidth  $D = 1$  and  $J=0$  (the case  $J \neq 0$  will be considered elsewhere).

Within LISA, the lattice model is exactly mapped onto its associated impurity problem supplemented with a self-consistency condition [5]. This approximation becomes exact in the limit of the dimensionality  $d \rightarrow \infty$  (or connectivity  $z \rightarrow \infty$ ). The resulting effective local action at a particular (any) lattice site reads, [14,5]

$$S_{loc} = \int_0^\beta \int_0^\beta d\tau d\tau' \sum_{\langle ij \rangle, a, \sigma} c_{a\sigma}^\dagger(\tau) \mathcal{G}_{a\sigma}^0{}^{-1}(\tau - \tau') c_{a\sigma}(\tau') + \frac{U}{2} \int_0^\beta d\tau \left( \sum_{i, a, \sigma} n_{ia\sigma} n_{ia-\sigma} + \sum_{i, a \neq b, \sigma} n_{ia\sigma} n_{ib-\sigma} + \sum_{i, a \neq b, \sigma} n_{ia\sigma} n_{ib\sigma} \right) \quad (2)$$

and the Weiss field  $\mathcal{G}_{a\sigma}^0$  is related to the local Green's function by the self-consistency condition,

$$\mathcal{G}_{a\sigma}^0{}^{-1}(i\omega) = i\omega + \mu - t^2 G_{a\sigma}(i\omega). \quad (3)$$

The LISA equations (2)-(3) have to be self-consistently solved for. In practice this is done by iteration. One begins with a guess for  $\mathcal{G}_{a\sigma}^0$  which is used in (2) to solve the many-body problem and calculate  $G_{a\sigma}$ . This is then used as input in (3) to get a new  $\mathcal{G}_{a\sigma}^0$  and the process is iterated until self-consistency is attained. Eq.2 also defines an *impurity problem* where the local site is coupled to an effective "conduction band" with hybridization function  $\Delta(i\omega) \equiv t^2 G_{a\sigma}(i\omega)$  similarly to the Anderson single impurity problem. This is the associated impurity problem within the LISA which has to be solved anew at each step of the iteration. To solve this *degenerate* impurity problem we use an extension of the HFQMC algorithm. The details for the implementation can be found in Ref. [8]. One of its salient features is the absence of the negative sign problem which allows the investigation of low temperatures ( $\sim 10^{-2}$  of the bandwidth). Converged solutions are typically obtained after 8 iterations using  $L = 64$  time slices in a few hours on a workstation.

We now turn to the discussion of the results from the solution of the LISA equations (2)-(3). In Fig.1 we show the total occupation number  $n = \langle n_{1\uparrow} + n_{1\downarrow} + n_{2\uparrow} + n_{2\downarrow} \rangle$  and its first derivative  $\kappa = dn/d\mu$  (which is proportional to the compressibility), as a function of the chemical potential  $\mu$ .

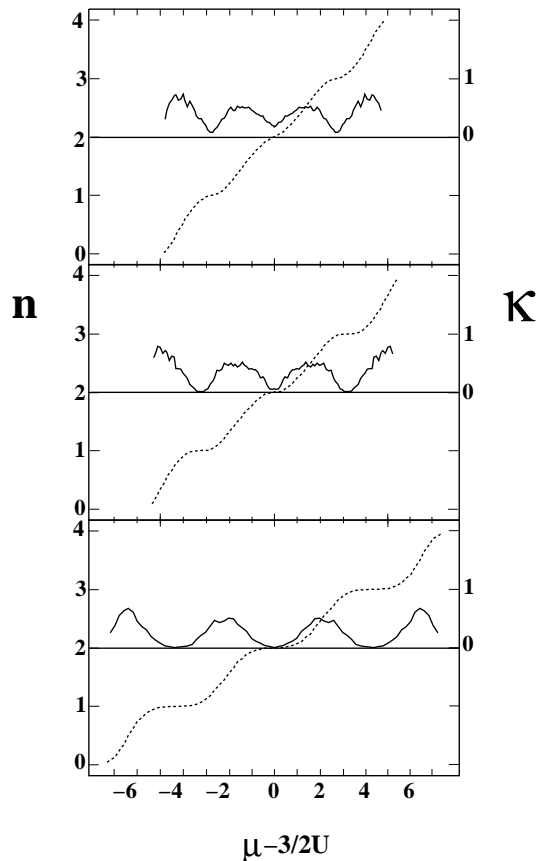


FIG. 1. Occupation number  $n$  and  $\kappa = dn/d\mu$  (dotted and solid curves) as a function of the chemical potential  $\mu$ .  $\kappa$  is obtained by numerical differentiation. The data are obtained at  $U = 2.5, 3, 4$  and  $T = 1/8$  (top to bottom). Note: for better comparison  $\mu$  is measured respect the particle-hole symmetry point at  $\frac{3}{2}U$ .

For  $U = 2.5$  we observe drops in  $\kappa$  at values of  $\mu$  corresponding to the integer fillings  $n = 1, 2, 3$  that indicates the onset of a correlated metallic state. This is demonstrated in Fig.2 where we plot the quasiparticle residue  $Z = (1 - \partial \text{Im}\Sigma / \partial \omega_n)^{-1}$  and the specific heat  $\gamma/\gamma_0 (= m^*/m_0$  in the  $d = \infty$  limit). We observe that as the system approaches the integer fillings the quasiparticles at the Fermi level become heavier as a consequence of the proximity to the MIT. On the other hand, at  $n = 0$  and 4 the quasiparticle residue approaches unity as the correlations vanish. It is worth noting the asymmetry in the behavior around  $n = 1$  and 3. As one approaches  $n = 1$  from below the specific heat diverges as the inverse of the doping  $\delta^{-1}$  ( $\delta = 1 - n$ ) [15]. However, as we approach  $n = 1$  from above the enhancement of  $\gamma/\gamma_0$  seems to be faster. The results for  $0 \leq n \leq 1$  are similar as the obtained within a one band model and gives a posteriori justification for its correct prediction of the behavior of  $\gamma/\gamma_0$  in  $La_{1-x}Sr_xTiO_3$  [12]. It would be interesting to test the asymmetry prediction of our model by approaching  $n = 1$  from above in oxygen deficient  $LaTiO_{3-y}$ . Around  $n = 2$ , which is the particle-hole

symmetry point, the enhancement of  $\gamma/\gamma_0$  is symmetric.

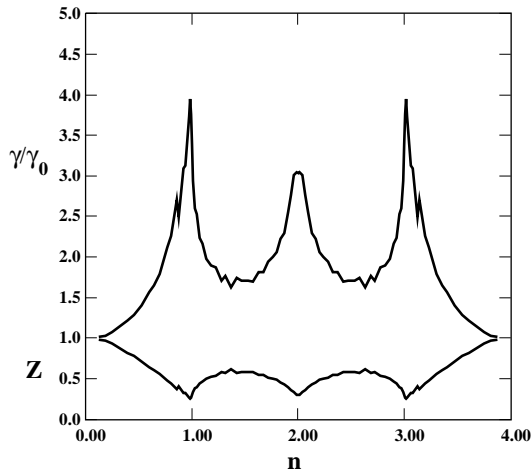


FIG. 2. Quasiparticle residue  $Z$  and specific heat  $\gamma/\gamma_0$  (bottom and top) as a function of the occupation number  $n$  obtained for  $U = 2.5$  and  $T = 1/8$ . We estimate the slope in the self-energy  $\Sigma$  as the ratio of  $\Sigma/\omega_n$  for the first Matsubara frequency. The wiggles are due to the QMC noise.

Back to Fig.1, we increase the value of the interaction strength to  $U = 3$ , and observe that the compressibility at  $n = 1$  and  $n = 3$  vanishes as the system goes through a metal insulator transition, [15] in fact,  $U_c(n = 1) = U_c(n = 3)$  due to particle-hole symmetry. On the other hand, the compressibility at  $n = 2$  also decreases but still remains finite, and the MIT is reached upon further increasing the interaction. Note that  $\kappa$  also goes to zero at the endpoints  $\mu - \frac{3}{2} \approx \pm 2U$ , but these are band insulating states which correspond to the completely empty  $n = 0$  and completely full  $n = 4$  state.

We find that the MIT of the degenerate model at  $n = 1, 2, 3$  have many features in common with the transition that occurs in the single band case [12]. In particular, at low enough temperature  $T \lesssim 0.04$  for  $n = 1, 3$  and  $T \lesssim 0.06$  for  $n = 2$ , and within a finite interval of the interaction  $U$  two distinct solutions coexist: one has metallic character while the other shows a gap at low frequencies. In Fig.3 we show for the two fillings  $n = 1$  and 2 the coexistent Green's functions obtained at  $T = 1/32$ . To select either solution within the coexistent region, one has to choose an appropriate “seed” at the beginning of the iteration. These Green's functions are obtained as a function of Matsubara frequencies, i.e., they live on the imaginary axis. In order to obtain the density of states they have to be analytically continued to the real axis. Nevertheless, the metallic or insulating nature of the solution can be unambiguously determined from their low frequency behavior. In fact, the metallic Green's function behaves as  $\text{Im}G(\omega) \neq 0$  for  $\omega \rightarrow 0$  and can be continuously connected to the non-interacting solution. On the other hand, the insulating Green's function shows linear behavior at small frequencies which is a signature of a

gap opening in the density of states; thus, in this case,  $\text{Im}G(\omega) \rightarrow 0$  for  $\omega \rightarrow 0$  and can be continuously connected to the atomic limit solution ( $t \rightarrow 0$ ).

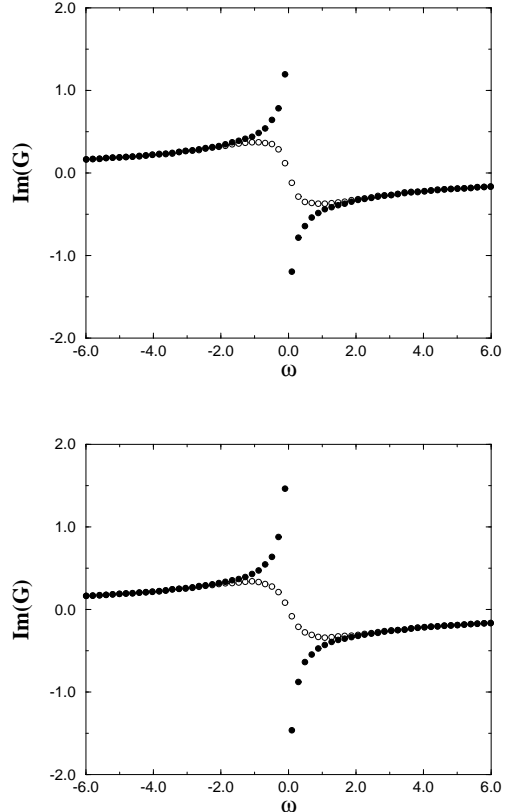


FIG. 3. Top: Imaginary part of the Green's function as a function of Matsubara frequency at  $T = 1/32$ ,  $U = 2.9$  and  $n = 1$ . The solid dots correspond to the metallic solution and the open dots to the insulating one. Bottom: Idem for  $T = 1/32$ ,  $U = 3.4$  and  $n = 2$ .

Calling  $U_{c1}(n)$  the minimum value of the interaction for which an insulating solution is allowed at given  $n$ , and  $U_{c2}(n)$  the maximum value for which a metallic solution is allowed; [12] we have established that at the lowest temperature investigated  $T = 1/32$ ,  $U_{c1}(1) = U_{c1}(3) \approx 2.8$ ,  $U_{c2}(1) = U_{c2}(3) \approx 3$  and  $U_{c1}(2) \approx 3.1$ ,  $U_{c2}(2) \approx 3.7$ . Using similar arguments as for the single band model, [16] one can demonstrate that at  $T = 0$  the metallic solution is lower in energy, thus, the  $T = 0$  MIT occurs at  $U_{c2}$  and is of second order. A direct consequence of two solutions being allowed in regions of the  $(U, T)$  plane at given integer fillings, is the existence of a first order transition line defined by the crossing of their free energies. This line starts at  $U_{c2}$  at  $T = 0$  and has a negative slope due to the large entropy of the insulating state, while at finite  $T$  it ends at another second order point where the two solutions eventually merge. These results are condensed into the phase diagram of Fig.4 which shows qualitative agreement with that of Ref. [10].

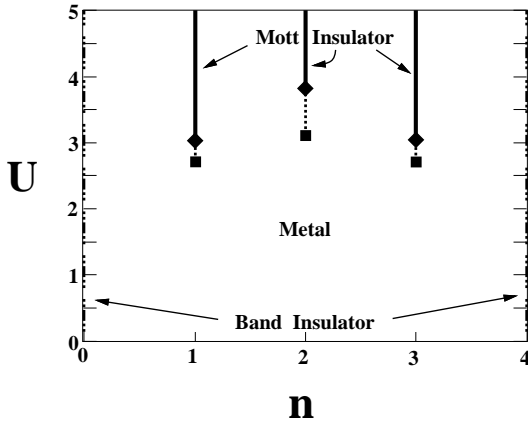


FIG. 4. Interaction  $U$  vs. filling  $n$  phase diagram for the paramagnetic solution. The 1<sup>st</sup> order transition lines at  $n = 1, 2, 3$  (dotted lines) end at 2<sup>nd</sup> order critical points. Diamonds indicate the approximate position of the  $T = 0$  critical points ( $U_{c2}$ ), and squares approximately indicate the finite  $T$  critical point where the two solutions merge ( $T(n = 1, 3) \approx 0.04$ ,  $T(n = 2) \approx 0.06$ ). Solid lines at  $n = 1, 2, 3$  indicate the Mott insulator states, and dashed-dotted lines at  $n = 0$  and 4 indicate the empty and full band insulator states.

From the experimental standpoint, it has been argued by Fujimori *et al.* [17] that the systematic analysis of the electronic properties of various transition metal oxide compounds with nominally *one electron* in a degenerate  $d$ -band shows evidence for a MIT due to electron correlations. Moreover, the extensively investigated  $V_2O_3$  compound contains nominally *two electrons* in a doubly degenerate  $e_g$  band and its phase diagram displays a paramagnetic MIT line which is *first order* [11]. Nevertheless, Castellani *et al.* [18] have argued that a relevant model for this system should contain just one electron in a doubly degenerate  $e_g$  band. In either case the qualitative physics is being correctly predicted by our results.

In conclusion, we obtain exact numerical solutions of the LISA mean field equations for the degenerate Hubbard model. These are exact solutions of the model in the limit of  $d = \infty$ . We find that within the paramagnetic phase the model has metal insulator transitions at the integer fillings  $n = 1, 2, 3$  which are similar in character as the single band case. In particular we find that  $U_c(n = 2) > U_c(n = 1) = U_c(n = 3)$ , and that there are regions in the  $(U, T)$  plane where two different solutions are allowed, one metallic and one insulating, which leads to a first order MIT line at finite temperatures. An important remark is that the observation of a similar scenario for the integer filling MIT in both, the single and degenerate band model, validates the often made assumption about the relevance of a single band Hubbard model for the qualitative investigation of compounds with narrow degenerate bands. This remark can be considered an a posteriori justification for the recent

success in the interpretation of low frequency spectroscopies of correlated systems with band degeneracy using a single band model [19,20]. However, the previous statement has to be taken with care as we have seen that some quantities, as for instance the specific heat, may show a different behavior depending how the MIT is approached.

Many interesting questions are open ahead, for instance, whether the present scenario is modified by the introduction of a finite  $J$  and the study of phases with long range order as function of  $U$ ,  $J$ ,  $T$  and  $n$ . These are certainly relevant questions for the understanding of the physics of transition metal oxides with partially filled  $d$ -bands.

Valuable conversations with A. Georges, I. H. Inoue, H. Kajueter and G. Kotliar are gratefully acknowledged.

- 
- [1] J. Kanamori, *Prog. Theor. Phys.* **30**, 275 (1963).
  - [2] P. Nozieres and A. Blandin, *J. Phys.* **41**, 193 (1980).
  - [3] K. I. Kugel and D. I. Khomskii, *Sov. Phys. JETP* **64**, 1429 (1973).
  - [4] M. Cyrot and C. Lyon-Caen, *J. Phys.* **36**, 253 (1975).
  - [5] A. Georges, G. Kotliar, W. Krauth and M. J. Rozenberg, to appear in *Rev. Mod. Phys.* (1996).
  - [6] D. Vollhardt, *Correlated Electron Systems*, ed. V. Emery (World Scientific, Singapore, 1993).
  - [7] J. E. Hirsch and R. M. Fye, *Phys. Rev. Lett.* **56**, 2521 (1986); H. Q. Lin and J. E. Hirsch, *Phys. Rev. B* **37**, 1864 (1988).
  - [8] K. Takegahara, *J. Phys. Soc. Jpn.* **62**, 1736 (1992).
  - [9] L. Dworin and A. Narath, *Phys. Rev. Lett.* **25**, 1287 (1970).
  - [10] A. Fujimori, *J. Phys. Chem. Solids* **53**, 1595 (1992).
  - [11] D. Mc Whan *et al.*, *Phys. Rev. B* **7**, 1920 (1973).
  - [12] M. J. Rozenberg, G. Kotliar and X. Y. Zhang, *Phys. Rev. B* **49**, 10181 (1994).
  - [13] A. Georges and W. Krauth, *Phys. Rev. B* **48**, 7167 (1993).
  - [14] A. Georges, G. Kotliar and Q. Si, *Int. J. Mod. Phys. B* **6**, 705 (1992).
  - [15] Similar results are obtained with a generalization of the IPT approach. H. Kajueter and G. Kotliar (private communication).
  - [16] G. Moeller, Q. Si, G. Kotliar, M. J. Rozenberg and D. S. Fisher, *Phys. Rev. Lett.* **74**, 2082 (1995).
  - [17] A. Fujimori, I. Hase, H. Namatame, Y. Fujishima, Y. Tokura, H. Eisaki, S. Uchida, K. Takegahara, and F. M. F. de Groot, *Phys. Rev. Lett.* **69**, 1796 (1992).
  - [18] C. Castellani, C. R. Natoli and J. Ranninger, *Phys. Rev. B* **18**, 4945 (1978).
  - [19] M. J. Rozenberg, G. Kotliar, H. Kajueter, G. A. Thomas, D. H. Rapkine, J. M. Honig and P. Metcalf, *Phys. Rev. Lett.* **75**, 105 (1995).
  - [20] M. J. Rozenberg, I. H. Inoue, H. Makino, F. Iga and Y. Nishihara, to appear in *Phys. Rev. Lett.*